Bioorganic & Medicinal Chemistry 19 (2011) 1002–1009

Contents lists available at ScienceDirect

Bioorganic & Medicinal Chemistry

journal homepage: www.elsevier.com/locate/bmc

In silico discovery of acylated flavonol monorhamnosides from *Eriobotrya japonica* as natural, small-molecular weight inhibitors of XIAP BIR3

Petra H. Pfisterer [a], Chenxi Shen [b], Zaneta Nikolovska-Coleska [b], Lilianna Schyschka [c], Daniela Schuster [d], Anita Rudy [c], Gerhard Wolber [d], Angelika M. Vollmar [c], Judith M. Rollinger [a], Hermann Stuppner [a,*]

[a] Institute of Pharmacy/Pharmacognosy and Center for Molecular Biosciences Innsbruck, University of Innsbruck, Innrain 52c, A-6020 Innsbruck, Austria
[b] Department of Pathology, Medical School, University of Michigan, 1301 Catherine Road, Ann Arbor, MI 48109-5602, United States
[c] Department of Pharmacy, Center for Drug Research, University of Munich, Butenandtstr. 5-13, D-81377 Munich, Germany
[d] Institute of Pharmacy/Pharmaceutical Chemistry and Center for Molecular Biosciences Innsbruck, University of Innsbruck, Innrain 52c, A-6020 Innsbruck, Austria

ARTICLE INFO

Article history:
Received 22 June 2010
Revised 14 October 2010
Accepted 16 October 2010
Available online 25 October 2010

Keywords:
Eriobotrya japonica
Molecular modeling
XIAP BIR3
Chemosensitizer

ABSTRACT

Targeting the baculoviral inhibitor of apoptosis proteins repeat (BIR) 3 of X-linked inhibitor of apoptosis proteins (XIAP) represents an innovative strategy for the design of chemosensitizers. Acylated flavonol monorhamnosides (AFMR) from *Eriobotrya japonica* Lindl. (Rosaceae) were virtually predicted as ligands of the XIAP BIR3 domain by using a previously generated pharmacophore model. From the methanol leaf extract of *E. japonica* an enriched mixture of AFMR was obtained showing chemosensitizing potential in combination with etoposide in XIAP-overexpressing Jurkat cells. The HPLC-SPE-NMR hyphenated technique facilitated the structure elucidation of three known and two new natural AFMR. The main constituent and virtual hit, kaempferol-3-*O*-α-L-(2″,4″-di-*E*-*p*-coumaroyl)-rhamnoside (**3**) was isolated from the enriched fraction. Applying a fluorescence polarization based binding assay, **3** was identified as XIAP BIR3 ligand with a dose-dependent affinity (IC_{50} 10.4 μM). Further, **3** induced apoptosis in XIAP-overexpressing Jurkat cells and activated caspase-9 in combination with etoposide. Docking experiments revealed a major impact of the coumaric acid and sugar moieties of **3** on XIAP BIR3 binding, which was experimentally confirmed. To conclude, this study elucidates **3** as natural, small-molecular weight XIAP BIR3 inhibitor using a combination of in silico and HPLC-SPE-NMR hyphenated techniques.

1. Introduction

Apoptosis is an essential cell suicide process that is of crucial importance for suppression of oncogenesis in multi-cellular organisms.[1] This process can be initiated by intristic or extrinsic pathways. The extrinsic pathway implicates the activation of death receptors. The intrinsic pathway is activated by extra-cellular cues and internal insults such as DNA damage, oxidative stress or signals induced by chemotherapeutic drugs. These events lead to the activation of the initiator caspase-9, a cysteine protease. The subsequent cascade of effector caspases results in the disassembly of the cell. This process can be inhibited by the members of the inhibitor of apoptosis protein (IAP) family, which are able to directly inhibit the caspases. At least eight distinct IAPs have been identified in the mammalian genome, each of which contains one to three copies of the baculoviral IAP repeat (BIR) domain. The best characterized family member X-linked IAP (XIAP), which is overexpressed in many tumors, binds and inhibits caspase-9 through its BIR3 domain.[2] This caspase-9 inhibition is neutralized by a mitochondrial protein named Smac/DIABLO (second mitochondria-derived activator of caspases/direct IAP-binding protein with low isoelectric point) by interacting directly with the XIAP BIR3 domain.[3]

The discovery of XIAP BIR3 ligands, so-called Smac-mimetics, is a promising strategy for the design of compounds modulating apoptosis pathways in chemoresistant cells in order to increase their sensitivity to conventional chemotherapeutic drugs (chemosensitizers). There are two major approaches, which have been attempted to discover Smac-mimetics. On the one hand, antisense oligonucleotides emerged as potentially useful agents: AEG 35156 reducing XIAP levels and sensitizing tumors to chemotherapy is currently under clinical assessment.[4,5] However, due to their limitations such as poor cell-permeability and in vivo stability, many groups focused on the discovery of small-molecular weight inhibitors of XIAP BIR3 on the other hand.[6–10]

In the field of natural products, embelin, a benzoquinone with an 11-carbon alkyl side chain originally isolated from the Japanese Ardisia herb (*Ardisia japonica*, Myrsinaceae), has been identified as XIAP BIR3 inhibitor.[10] For thousands of years, natural products have played a crucial role in the discovery and development of pharmaceuticals. Today, they are still a significant source of novel drugs, especially in the field of anti-cancer therapeutics.[11] In the

* Corresponding author. Tel.: +43 512 507 5300; fax: +43 512 507 2939.
E-mail address: Hermann.Stuppner@uibk.ac.at (H. Stuppner).

0968-0896/$ - see front matter © 2010 Published by Elsevier Ltd.
doi:10.1016/j.bmc.2010.10.046

time frame from the 1940s to 2006, 73% of the 155 small molecules approved as anti-cancer drugs are naturally derived agents, with 47% being either natural products or their derivatives.[12] This success is based on their biosynthesis by numerous enzymes and co-evolvement with the requirements of ligand functionality.[13,14] The identification of embelin as XIAP BIR3 inhibitor has been enabled by a computational structure-based database search using the docking software DOCK. Whereas molecular modeling is well established as an important and successful method to discover and rationalize bioactivities in medicinal chemistry, its application has proven to be also a powerful tool to exploit the natural products' bioactivities.[15] Recently, natural products as molecular cancer therapeutics discovered or rationalized by molecular modeling have been reviewed.[16]

In this study, kaempferol-3-*O*-α-L-(2″,4″-di-*E*-*p*-coumaroyl)-rhamnoside (**3**) has been identified as a natural, small-molecular weight XIAP BIR3 inhibitor using (i) virtual screening of a focused 3D multi-conformational natural product database with a generated pharmacophore model of the XIAP BIR3 binding groove as search query and (ii) docking experiments to rationalize the impact of substructures on bioactivity.

2. Results and discussion

2.1. Description of pharmacophore model Hypo2-1TFQexcludvolumes7

The pharmacophore model Hypo2-1TFQexcludedvolumes7 consists of two donor features describing the ligand's peptide nitrogens which are supposed to bind to the amino acids Thr308 and Gly306, respectively. Furthermore, a hydrogen acceptor function was localized from the Trp323 to the ligand's N-terminal peptide oxygen. The three hydrophobic features mimic the bulky *tert*-butyl residue of the ligand, its proline ring, and its 1,2,3,4-tetrahydronaphthalene, respectively. Additionally, excluded volume spheres representing side chains of the protein and therefore inaccessible areas for the ligand have been included in the model.

2.2. Establishment and in silico screening of a natural product database

Loquat or *Eriobotrya japonica* (Thunb.) Lindl. from the Rosaceae family is an ornamental tree native to South China and Japan. It is also cultivated in Europe since the 18th century due to its delicious fruits. The leaves are used in Traditional Chinese Medicine for the treatment of bronchitis, cough, fever, and nausea. In literature, constituents of the leaves, especially polyphenols and triterpene acids, are reported as being cytotoxic or showing anti-cancer properties in vitro and in vivo.[17–20] Although information concerning the down-regulation or suppression of XIAP is available for some constituents such as (−)-epigallocatechin-3-gallate (EGCG), kaempferol and ursolic acid, no ligands of the XIAP BIR3 groove have been reported yet.[21–24] *E. japonica* has been selected as plant material for this study due to (i) its long-term use as medicinal plant, (ii) its pharmacological profile described in literature, and (iii) its availability.

In order to identify potential XIAP BIR3 inhibitors, a 3D multi-conformational database of the known constituents from the leaves of *E. japonica* has been established and labelled as ERIO. Using the pharmacophore model Hypo2-1TFQexcludedvolumes7 as search query, this database, which consists of 121 compounds, was virtually screened resulting in 35 hits (28.9%). The acylated flavonol monorhamnosides emerged as one of the most promising phytochemical classes, because they all mapped all the features of the pharmacophore model (100%). Based on the finding that the model found only 14% of the flavonoid glycosides, we assume that acylation of the molecules has an influence on the mapping results and consequently also on bioactivity. Therefore, this interesting phytochemical class has been selected for further investigations.

2.3. Enrichment of acylated flavonol monorhamnosides

Fractionation of the methanol crude extract by silica gel and Sephadex LH-20 column chromatography resulted in an enriched acylated flavonol monorhamnoside (eAFMR) fraction. To facilitate the structural characterization of the main compounds of this complex mixture, the HPLC-SPE-NMR hyphenated technique was employed. By applying mass spectrometry, 1D and 2D NMR experiments and comparison with data from literature,[25] three compounds have been identified as kaempferol-3-*O*-α-L-(3″-*Z*,4″-*E*-di-*p*-coumaroyl)-rhamnoside (**1**), kaempferol-3-*O*-α-L-(3″,4″-di-*E*-*p*-coumaroyl)-rhamnoside (**2**), and kaempferol-3-*O*-α-L-(2″,4″-di-*E*-*p*-coumaroyl)-rhamnoside (**3**) (Fig. 1). In literature, compound **1** is described as having been isolated from *Epimedium sagittatum* as well as being instable becoming a mixture of six acylated flavonol monorhamnosides via isomerization and *trans*-esterification after storage overnight.[25,26] Compounds **2** and **3** have been isolated from various plant materials including *Machilus philippinensis*, *E. sagittatum*, and *Laurus nobilis*,[25–27] whereas compounds **1** and **2** have not been isolated before from *E. japonica*. Additionally, a mixture of two compounds (**4** and **5**), which had been trapped together, could be assigned to novel acylated flavonol monorhamnosides (Fig. 1). To our best knowledge, these compounds are described for the first time. The LC-HR-ESI-MS (positive mode) of compounds **4** and **5** showed $[M+Na]^+$, $[M+H]^+$, and $[M+K]^+$ at *m/z* 777.1803, 755.1988, and 793.1533, respectively, suggesting an additional methoxy group for each compound in respect to **1**–**3**. Integration of the signals of the ^1H NMR spectrum revealed the ratio of the mixture (5:3) and facilitated the assignment of the NMR signals to the compounds. Furthermore, the spectrum displayed signals for two kaempferol moieties, an AX system for H-6 (δ 6.26, d, J = 1.8) and H-8 (δ 6.45, d, J = 1.8) and an AA′XX′ system for H-2′ (H-6′, δ 7.85, d, J = 8.4) and H-3′ (H-5′, δ 7.06 and 7.07, d, J = 8.4), two rhamnopyranosyl moieties ($\delta_{H\text{-}1''}$ 5.72 and 5.74, d, J = 1.8; $\delta_{H\text{-}6''}$ 0.85, d, J = 6.6), two *E*-coumaroyl moieties and two *E*-feruloyl moieties ($J_{H\text{-}2'''/H\text{-}3'''}$ = 16.2, $\delta_{H\text{-}10'''}$ 3.91 and 3.94, s). In respect to the protons of a non-substituted rhamnose, the signals of H-2″ and H-4″, analyzed by the COSY spectrum, were down-field shifted in both compounds. In accordance to literature data of the chemical shifts of H-2‴ and H-3‴,[25,28] compounds **4** and **5** could be assigned to kaempferol-3-*O*-α-L-(2″-*E*-feruloyl,4″-*E*-p-coumaroyl)-rhamnoside and kaempferol-3-*O*-α-L-(2″-*E*-*p*-coumaroyl,4″-*E*-feruloyl)-rhamnoside, respectively (Table 1).

Comparing the HPLC analysis of eAFMR with a fresh methanol crude extract from the leaves of *E. japonica* revealed compounds **3**, **4**, and **5** being genuine in the plant material, and suggested compounds **1** and **2** being artefacts. Probably, the latter ones are isomers of labile genuine constituents yielded during the isolation process. Compound **3** was the only constituent which showed reasonable stability, whereas the others became a mixture when stored over night.[25] Therefore, assessment of chemosensitizing effects was performed with the mixture eAFMR containing compounds **1**–**5** and the isolated compound **3**.

2.4. Determination of chemosensitizing activity

For pre-evaluation of cytotoxicity, a range of different concentrations of eAFMR was measured by the MTT assay in wild type Jurkat cells (data not shown). Based on these data, the concentration interval for a 90% cell-viability was determined for eAFMR with approximately 5 μg/mL.

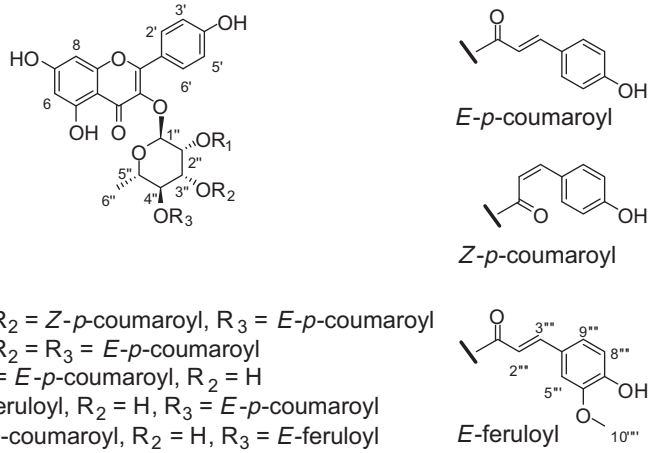

Figure 1. Structural formula of identified acylated flavonol monorhamnosides from the leaves of *E. japonica*.

Table 1
^{1}H and ^{13}C NMR spectroscopic data of compounds **4** and **5** (600 MHz, CD_3CN)

Carbon No.	**4**		**5**	
	^{1}H[a]	^{13}C	^{1}H[a]	^{13}C
Kaempferol moiety				
6	6.26 (d, 1.8)	99.6	6.26 (d, 1.8)	99.6
8	6.45 (d, 1.8)	94.7	6.45 (d, 1.8)	94.7
2′, 6′	7.85 (d, 8.4)	131.9	7.85 (d, 8.4)	131.9
3′, 5′	7.06 (d, 8.4)	116.5	7.07 (d, 8.4)	122.9
Rhamnose moiety				
1″	5.72 (d, 1.8)	98.5	5.74 (d, 1.8)	98.5
2″	5.49 (m)	72.3	5.49 (m)	72.3
3″	4.07 (m)	68.1	4.07 (m)	68.1
4″	4.89 (t, 9.6)	74.3	4.89 (t, 9.6)	74.3
5″	3.27 (m)	69.4	3.27 (m)	69.4
6″	0.85 (d, 6.6)	17.4	0.85 (d, 6.6)	17.4
	2″-*E*-Feruloyl moiety		4″-*E*-Feruloyl moiety	
2‴	6.47 (d, 16.2)	115.3	6.34 (d, 16.2)	115.7
3‴	7.66 (d, 16.2)	146.6	7.53–7.60[b]	146.1
5‴	7.27 (d, 1.8)	111.5	7.28 (d, 1.8)	111.5
8‴	6.86 (d, 8.4)	116.5	6.88 (d, 8.4)	116.5
9‴	7.13 (dd, 1.8, 8.4)	124.5	7.17 (dd, 1.8, 8.4)	123.9
10‴	3.91 (s)	56.7	3.94 (s)	56.7
	4″-*E*-Coumaroyl moiety		2″-*E*-Coumaroyl moiety	
2‴	6.30 (d, 15.6)	115.7	6.42 (d, 15.6)	114.9
3‴	7.53–7.60[b]	146.1	7.68, (d, 15.6)	146.6
5‴, 9‴	7.53–7.60[b]	131.3	7.53–7.60[b]	131.3
6‴, 8‴	6.85–6.90[b]	116.3	6.85–6.90[b]	116.5

[a] Coupling constants (*J* values in Hz) in parentheses.
[b] Signal patterns are unclear due to overlapping.

Using the Nicoletti assay, eAFMR was tested in XIAP-overexpressing Jurkat cells for its chemosensitizing potential (Fig. 2A). Whereas 5 μg/mL eAFMR caused only weak effects itself (1.6% apoptotic cells), its combination with 1 μM etoposide strongly induced cell death (37.5% apoptotic cells) suggesting a synergistic effect of eAFMR and etoposide.

The activation of the initiator caspase-9 was elucidated by western blot analysis. As shown in Fig. 2B after 48 h stimulation eAFMR in combination with etoposide caused an activation of caspase-9 in XIAP-overexpressing Jurkat cells. At this time point etoposide alone does not affect the cleavage of the caspase.

2.5. Virtually predicted binding interactions

Screening the ERIO database with the pharmacophore model Hypo2-1TFQexcludedvolumes7 as search query, compound **3** emerged as virtual hit. As compounds **1**, **2**, **4**, and **5** have been identified from the leaves of *E. japonica* for the first time during this study, these compounds were not present in the ERIO database. Therefore, they were mapped into the pharmacophore model revealing compound **1** also as virtual hit. Since compound **1** was described as being chemically instable,[25] no further modelling experiments were performed on this structure. In order to get further insights into the possible binding mode of the virtual hit **3**, it was docked into PDB complex 2JK7 (X-ray structure of XIAP BIR3 bound to a Smac mimetic),[8] using CCDCs software GOLD.[29] GOLD implements a genetic algorithm for flexible ligand placement in protein binding sites. The most relevant docking pose was selected by (i) automatically generating a 3D pharmacophore using the program LigandScout 2.0[30,31] and (ii) subsequent scoring according to the geometric fit of the relevant interactions. The chemical features used for this workflow are shown in Fig. 3. The set of

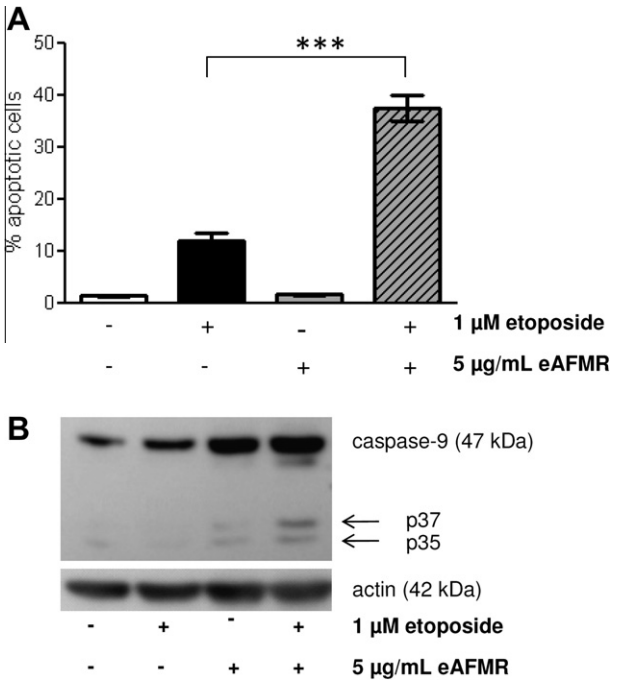

Figure 2. (A) Testing of eAFMR for its chemosensitizing potential in XIAP-overexpressing Jurkat cells towards etoposide-induced apoptosis (data are the mean ± SEM of three independent experiments performed in triplicate, 24 h stimulation). *** P <0.001, analysis of variance (ANOVA/Bonferroni). (B) After 48 h treatment eAFMR in combination with sub-toxic doses of etoposide activates caspase-9 in XIAP-overexpressing Jurkat cells. Cleavage products which indicate active caspase-9 are shown by arrows. Actin was used as loading control. A representative experiment out of two independent experiments is shown.

interactions includes hydrogen bonds with Gly306, Leu307, and Thr308, and a π-cation interaction with Lys297. Additionally, hydrophobic contacts with Leu307, Trp310, Ly297, and Trp323 can be observed.

The results of the docking experiment show a possible binding mode of compound **3** (Fig. 4), where the sugar moiety replaces the central ring system in the Smac mimetic compound allowing the carbonyl oxygen of the ester moiety to form a hydrogen bond acceptor interaction with Thr308. The hydroxyl moiety in 3″ position possibly interacts with Gly306 to form a hydrogen bond donor (similar as the amide moiety in the Smac mimetic) and at the same time acts as an H-bond acceptor with Tyr324. Further common interactions observed are the π-cation interaction with Lys297. The placement of compound **3** in the XIAP BIR3 binding site suggests a similar location of hydrophobic areas. To illustrate the spatial arrangement of lipophilic areas between ligands and protein, Fig. 5 shows both the Smac mimetic and compound **3** overlaid on the protein surface, which is coloured by hydrophobicity.

2.6. XIAP BIR3 inhibiting activity and assessment of structural requirements

To evaluate the proposed bioactivity, we isolated compound **3**, because it is one of the main constituents of eAFMR and was not yet described as being instable in contrast to the virtual hit **1**.[25] The isolation of **3** was achieved by means of preparative HPLC starting from eAFMR. Before testing **3** in the fluorescence polarization based binding (FP) assay, its stability was investigated under FP test conditions, and was found to be stable. The mixture eAFMR (calculated with an average molecular weight of 725) and compound **3** showed similar binding affinities to the XIAP BIR3 groove with IC_{50} values of 11.7 and 10.4 µM, respectively, revealing **3** as a constituent of eAFMR with a representative XIAP BIR3 inhibiting activity (Fig. 7). As shown in Fig. 8A compound **3** is able to induce apoptosis in combination with etoposide in XIAP-overexpressing Jurkat cells. Also caspase-9 is activated upon stimulation with compound **3** and sub-toxic dosis of etoposide (Fig. 8B).

For the assessment of all the virtually predicted interactions of compound **3** within the XIAP BIR3 binding site, the impact of the

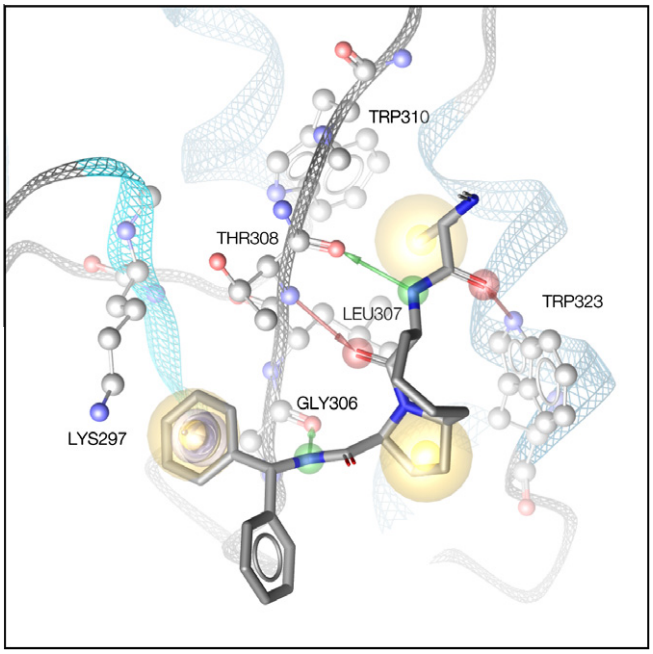

Figure 3. 3D pharmacophore showing the relevant interactions of PDB complex 2JK7 (Smac mimetic bound to XIAP BIR3). Hydrophobic areas are shown as yellow spheres, hydrogen bond donors and acceptors as green and red arrows, respectively, and aromatic interactions as purple tori.

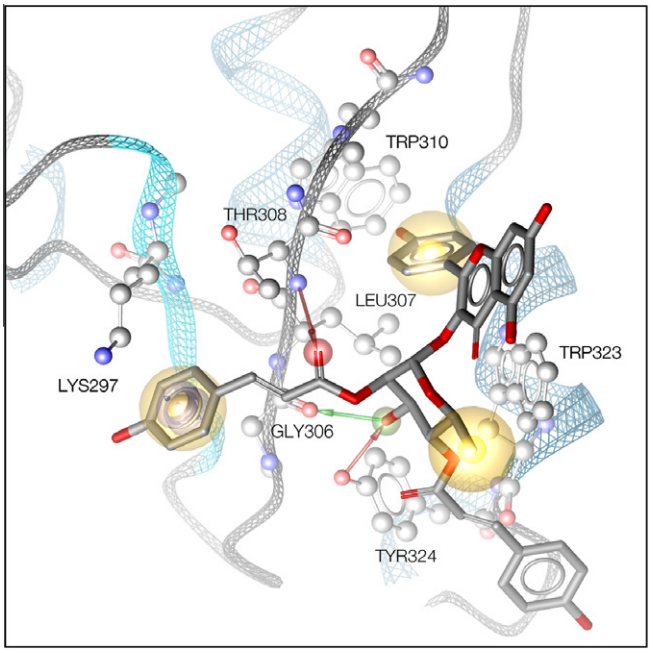

Figure 4. Assumed interactions of compound **3** after docking into PDB complex 2JK7. Hydrophobic areas are shown as yellow spheres, hydrogen bond donors and acceptors as green and red arrows, respectively, and aromatic interactions as purple tori.

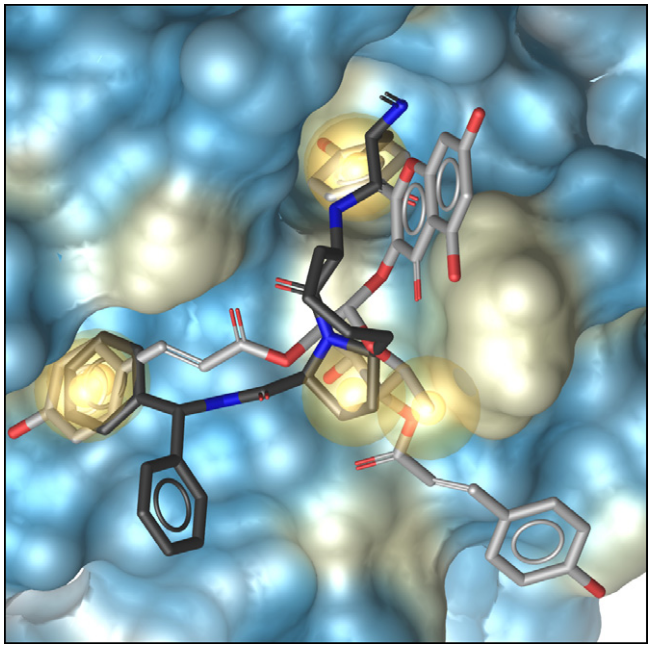

Figure 5. Hydrophobic contacts with the XIAP BIR3 protein surface. Blue surface colouring indicates polar areas, while yellow corresponds to hydrophobic areas. Yellow spheres located on the ligand side illustrate hydrophobic chemical feature locations as detected by LigandScout. Compound **3** carbon atoms are shown in light gray, the ones of the Smac mimetic compound (2JK7) in dark gray.

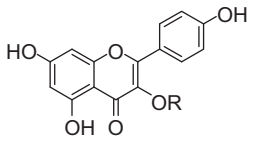

6 R = α-L-rhamnose
7 R = H

Figure 6. Structural formula of kaempferol-3-*O*-α-L-rhamnoside (**6**) and kaempferol (**7**).

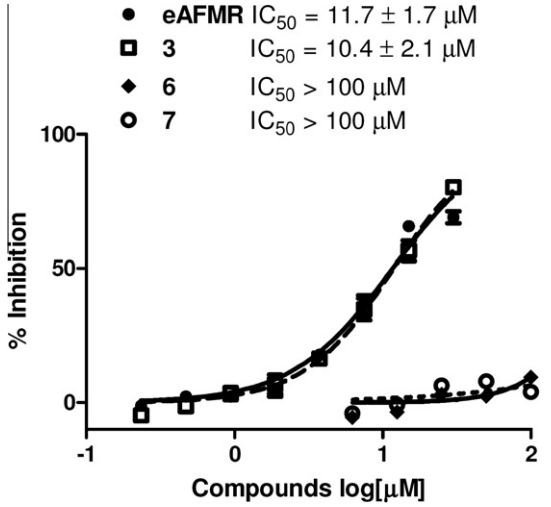

Figure 7. Competitive binding curves of eAFMR and compounds **3**, **6**, and **7** to the XIAP BIR3 protein determined by the FP assay.

acid and sugar moieties on the bioactivity was evaluated. Therefore, kaempferol-3-*O*-α-L-rhamnoside (**6**) yielded by alkaline

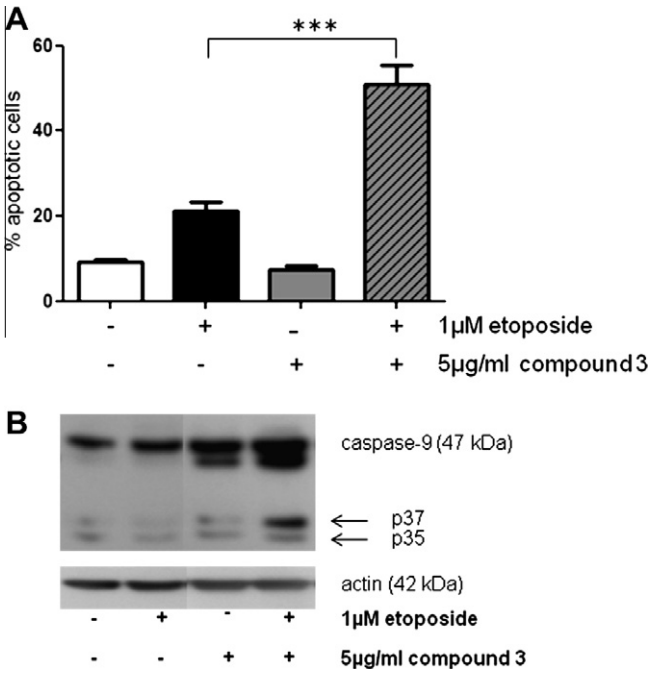

Figure 8. (A) Testing of compound **3** for its chemosensitizing potential in XIAP-overexpressing Jurkat cells towards etoposide-induced apoptosis (data are the mean ± SEM of three independent experiments performed in triplicate, 48 h stimulation). *** P <0.001, analysis of variance, (ANOVA/Bonferroni). (B) After 48 h treatment compound **3** in combination with sub-toxic doses of etoposide activates caspase-9 in XIAP-overexpressing Jurkat cells. Cleavage products which indicate active caspase-9 are shown by arrows. Actin was used as loading control. A representative experiment out of two independent experiments is shown.

hydrolysis of eAFMR, and the underlying flavonol moiety, kaempferol (**7**) (Fig. 6), have been subjected to experimental investigation using the FP assay. They did not abrogate the interaction between the Smac peptide and the XIAP BIR3 protein (IC_{50} values over 100 μM for both compounds, Fig. 7). Both compounds are constituents from the leaves of *E. japonica*.[32,33]

3. Conclusion

In the search for natural compounds binding to the XIAP BIR3 groove, the medicinal plant *E. japonica* emerged as promising plant material. Applying a virtual screening of a 3D multi-conformational database of all its known constituents with the pharmacophore model of the XIAP BIR3 groove as search query, acylated flavonol monorhamnosides have been identified as promising phytochemical class. Experimental investigations confirmed the in silico results elucidating **3** as small-molecular weight XIAP BIR3 inhibitor with an IC_{50} value of 10.4 μM. Whereas anti-inflammatory, anti-bacterial, and anti-diabetic activities of **3** are described in literature,[25,34–36] no anti-cancer activity has been reported so far.

Compound **3** is one of the main constituents of eAFMR, which has shown chemosensitizing potential in XIAP-overexpressing Jurkat cells and a binding affinity to the XIAP BIR3 groove with an IC_{50} value of 11.7 μM. The similar IC_{50} values of **3** and eAFMR suggest that the other constituents of eAFMR have comparable binding affinities to the XIAP BIR3 groove as compound **3**. Applying the HPLC-SPE-NMR hyphenated technique, it was possible to assign five constituents, among them two new ones, demonstrating that this technique is useful to identify single compounds in a complex mixture and to disclose even artefacts of labile natural products. Furthermore, the combination of HPLC-SPE-NMR and in silico techniques offered an insight into possible ligand-target interactions of single compounds in complex mixtures.

The results of the docking experiments suggested an impact of the sugar and coumaric acid moieties of compound **3** on its bioactivity. For the assessment of these virtually predicted interactions, compounds **6** and **7** have been evaluated by the FP assay showing no binding activity to the XIAP BIR3 domain. Although compound **6** is described in literature as showing anti-cancer and cytotoxic activities,[37] the mechanism could not be elucidated yet. Compound **7** has been isolated from many plant sources such as tea, broccoli, and leeks, and is therefore abundant in our diet.[38] In literature, it is reported as showing anti-cancer activity[39,40] and as potentiating the effects of chemotherapeutic agents like cytarabine, doxorubicin, and tumor necrosis factor-related apoptosis-inducing ligand (TRAIL).[41–43] Concerning the underlying mechanism of these chemosensitive effects, the amplification of reactive oxygen species (ROS) toxicity and the up-regulation of death receptor (DR) 4 and 5 is described.[42,43] Although compound **7** down-regulates the expression of XIAP,[22,23] a binding to the XIAP BIR3 groove can be excluded based on our investigations.

To conclude, this study exemplarily shows the benefit of molecular modelling for the discovery and rationalization of bioactive natural products in the field of anti-cancer therapy.

4. Experimental

4.1. Generation of pharmacophore model Hypo2-1TFQexcludedvolumes7

As starting point the Protein Data Bank entry 1TFQ, which represents a NMR-structure of an antagonist of the XIAP-caspase-9-interaction complex to the BIR3 domain of XIAP was used.[44,45] The information was merged with interactions from the more recent crystal structure 2JK7[8] and data from SAR studies[46,47] revealing essential ligand-target interactions. A 3D pharmacophore model was implemented in a pharmacophore model using the Catalyst Software package (version 4.11, Accelrys Inc., San Diego, CA). Exclusion volume spheres representing side chains of the protein and therefore inaccessible areas were included to complete the pharmacophore model. Before using the generated pharmacophore model as virtual screening search query, the hypothesis was successfully validated by its ability to retrieve all compounds of a multi-conformational database consisting of 30 compounds known to inhibit XIAP BIR3.

4.2. Multi-conformer generation and virtual screening of natural product database

3D models of 121 reported constituents from the leaves of *E. japonica* were built using the structure editor within the Catalyst Software Package (version 4.11, Accelrys Inc., San Diego, CA) installed on a standard personal computer equipped with an Intel Core 2 Duo processor (2.13 GHz; 1 GB RAM) running Fedora Core 6 Linux. Compounds were minimized using the default parameters of the CHARMM force field in order to reduce internal strain energy. Multi-conformational models were generated by randomized conformational analysis using the Poling algorithm[48,49] and stored in a binary database using the CatDB procedure within Catalyst (BEST algorithm for conformer generation; maximum of conformers: 250).

4.3. Docking

Docking was performed using the software GOLD V4.0 (available from the Cambridge Crystallographic Data Centre, CCDC, Cambridge, UK) with the graphical user interface Hermes for protein and docking setup. For docking all default values were used, and 50 different docking poses were generated. The ligand was prepared using LigandScout version 2.0 (available from Inte:Ligand GmbH, Vienna, Austria). Redocking experiments of the original ligand reproduced the experimentally determined geometry of the Smac mimetic compound from 2JK7 with an RMSD value below 0.9A.

To rank the resulting poses, an automatic 3D pharmacophore for complex 2JK7 was generated and the generated poses for compound **3** were ordered according to their geometric chemical feature overlap of the interaction pattern derived from the PDB complex.

4.4. General experimental procedures

All chemicals were analytical grade. Solvents were either analytical grade or puriss. grade and distilled before use. Optical rotation was measured on a Perkin Elmer 341 polarimeter (Wellesley, MA) at 20 °C. Column chromatography (CC) was performed under TLC monitoring using silica gel (silica gel 60, 40–63 μm; VWR, Darmstadt, Germany) and Sephadex LH-20 (20–100 μm, Pharmacia Biotech, Uppsala, Sweden). TLC was performed on silica gel 60 F_{254} plates (0.25 mm; VWR, Darmstadt, Germany), mobile phase: dichloromethane/methanol, 9:1 (v/v), and detected with vanillin/H_2SO_4 (1% w/v and 5% v/v methanolic solutions, respectively). HPLC-data were obtained on a Hewlett-Packard-(HP)-1100 system (Agilent, Waldbronn, Germany), equipped with a photodiode array detector (DAD), column thermostat and auto sampler. The LC was fitted with a Phenomenex Polar RP, 4 μm, 150 × 4.60 mm at a column temperature of 60 °C, flow rate 0.8 mL/min, injection volume 10 μL, using DAD (270, 320 nm). The mobile phases consisted of A: bidistilled water, B: acetonitrile (Merck 1.00030.2500): 25% methanol (Merck 1.06007.2500): 0.1% formic acid (98–100%, Merck 832 K10599664) (v/v/v); gradient: 0 min 40% B, 20 min 60% B, 21 min 98% B, 30 min 98% B. For LC-ESI-MS experiments the HPLC was coupled to a Bruker Esquire 3000^{plus} ion trap mass spectrometer (Bruker Daltonics, Bremen, Germany); MS-parameters: split 1:5; ESI alternative mode; spray voltage: 4.5 kV; dry gas: N_2, 6.0 L/min, 350 °C; nebulizer: 30 psi; scanning range: 100–1500 *m/z*. For LC-HR-ESI-MS experiments the HPLC was coupled to a Bruker micrOTOF-Q II mass spectrometer (Bruker Daltonics, Bremen, Germany); HR-MS parameters: split 1:3; ESI positive mode; spray voltage 4.5 kV; dry gas: N_2, 6.0 L/min, 200 °C; nebulizer: Ar, 22 psi; scanning range: 150–1000 *m/z*. For investigation of stability under FP test conditions, compound **3** was dissolved in 15 μL dimethyl sulfoxide and 360 μL phosphate buffer (100 mM, pH 7.5) were added to obtain a final volume of 375 μL. The solution was analyzed by HPLC at $t = 0$, 1.5, and 3 h. The chromatographic peaks were integrated and the relative percentage of the area at each time was calculated.

4.5. HPLC-SPE-NMR experiments

eAFMR was separated on a Hewlett-Packard-(HP)-1200 system (Agilent, Waldbronn, Germany), equipped with an online degaser, autosampler, UV, and a quaternary pump. The LC was fitted with a Phenomenex Polar RP, 4 μm, 150 × 4.60 mm at a column temperature of 60 °C, flow rate 0.8 mL/min, injection volume 10 × 20 μL. The mobile phases consisted of A: bidistilled water, B: acetonitrile (Merck 1.00030.2500): 25% methanol (Merck 1.06007.2500): 0.1% formic acid (98–100%, Merck 832 K10599664) (v/v/v); gradient: 0 min 2% B, 11 min 2% B, 12 min 43% B, 40 min 43% B, 42 min 98% B, 55 min 98% B. The post-column eluent was mixed with water supplied by a make-up pump (1.3 mL/min), before peak trapping on Hysphere-Resin GP cartriges (10–12 μm) using the SPE system Prospekt. The loaded cartridges were flushed with dry N_2 gas for 50 min, and the analyte was transferred to a Bruker

Avance II 600 spectrometer (Bruker Biospin, Rheinstetten, Germany) with CD_3CN (30 μL NMR probe). The NMR spectra were calibrated to the residual non-deuterated solvent signal. Mass, 1D and 2D NMR spectroscopic data of compounds **1**, **2**, and **3** have been in accordance with literature.[25] Compounds **4** and **5**: UV (acetonitrile–H_2O) λ_{max} nm: 265, 320; LC-HR-ESI-MS (positive mode) *m*/*z* 777.1803 $[M+Na]^+$ (cal. for $C_{40}H_{34}NaO_{15}^+$, 777.1790), *m*/*z* 755.1988 $[M+H]^+$ (cal. for $C_{40}H_{35}O_{15}^+$, 755.1970), *m*/*z* 793.1533 $[M+K]^+$ (cal. for $C_{40}H_{34}KO_{15}^+$, 793.1529); for ^1H and ^{13}C NMR see Table 1.

4.6. Material

Authenticated leaves of *E. japonica* (Thunb.) Lindl. were collected in the Botanical Garden of Innsbruck. A voucher specimen (JR-20061023-A1) was deposited in the Herbarium of the Institute of Pharmacy/Pharmacognosy, Leopold-Franzens University of Innsbruck, Austria.

Kaempferol (**7**) has been purchased from Sigma Aldrich (Vienna, Austria) with a HPLC-purity ⩾96%.

Human leukemia Jurkat T cells (wild type Jurkat clone J16, S-Jurkat) were obtained from H. Walczak and P.H. Krammer (Heidelberg, Germany); XIAP-overexpressing Jurkat cells were kindly provided by C. Duckett (Ann Arbor, Michigan, USA).[50] Both cell lines were cultured (37 °C, 5% CO_2) in RPMI 1640 containing 2 mM L-glutamine supplemented with 10% FCS gold (PAA Laboratories GmbH, Linz, Austria) and 1% pyruvate (Sigma, Deisenhofen, Germany). Medium of transfected cells was supplemented with 1 μg/mL puromycin (PAA Laboratories GmbH, Linz, Austria) every fifth passage. Etoposide was purchased from Merck Biosciences (Darmstadt, Germany), propidium iodide from Sigma (Deisenhofen, Germany).

4.7. Extraction and isolation

550 g of the air-dried and milled leaves of *E. japonica* were extracted with 1600 mL dichloromethane three times for 24 h at room temperature. The plant material was filtered off and the solvent was evaporated under reduced pressure to afford 11.9 g dichloromethane crude extract. In the same way, the remaining plant material was then extracted three times with 1800 mL methanol yielding 45.1 g methanol crude extract. 27 g of the methanol crude extract were fractionated using a silica gel CC (310 g, 5 × 35 cm) with 400 mL step gradients from dichloromethane to methanol to yield 11 fractions (A1-A11). Fraction A4 (649 mg) was subjected to Sephadex CC (3.5 × 70 cm) using methanol as mobile phase to afford 7 fractions (B1-B7). Fraction A5 (828 mg) was fractionated using silica gel CC (310 g, 3.5 × 30 cm) with 200 mL step gradients from dichloromethane to methanol yielding 10 fractions (C1–C10). 30 mg of fraction C6 were fractionated by a liquid/liquid distribution (water/chloroform/methanol, 2:4:3, v/v/v) to gain two fractions (D1 and 2). HPLC analysis revealed B7 (19.4 mg) and D1 (7.9 mg) as being enriched fractions of acylated flavonol monorhamnosides. In the same way, 18 g of the methanol crude extract were fractionated yielding two fractions containing acylated flavonol monorhamnosides (12.8 and 23.1 mg). Due to their similar HPLC patterns the four enriched fractions of acylated flavonol monorhamnosides have been combined and labelled as eAFMR (63.2 mg).

10 mg of eAFMR were subjected to preparative HPLC (Xterra® MS C18, 7.8 × 100 mm, 5 μm, Waters), eluted with acetonitrile/bidistilled water (38:62, v/v), flow rate 3 mL/min to give 4.2 mg of compound **3** (47.4–52.8 mL elution volume; optical rotation $[\alpha]_D^{20}$ −38.0° (methanol, *c* 0.08); ESI-MS (negative mode): 723.7 $[M-H]^-$; 1D NMR data in accordance with literature;[25] HPLC-purity ⩾95%), which was purified by filtration over a SPE cartridge (Strata C18-E, 55 μm, 70 Å, Phenomenex).

4.8. Alkaline hydrolysis of eAFMR

25 mg of the mixture eAFMR were dissolved in 5% NaOH (27 mL) and incubated at room temperature for 15 h. The reaction mixture was neutralized with 10% H_2SO_4 and subjected to extraction with ethyl acetate. The ethyl acetate layer was evaporated to dryness and purified over Sephadex LH-20 CC (1 × 35 cm) using methanol as mobile phase to afford 5.4 mg of compound **6** (optical rotation $[\alpha]_D^{20}$ −83.6° (methanol, *c* 0.54); ESI-MS (negative mode): *m*/*z* 431.8 $[M-H]^-$, 863.1 $[2\,M-H]^-$; 1D and 2D NMR data in accordance with literature;[51] HPLC-purity ⩾95%).

4.9. Pharmacological testing

Before application, the mixture was dissolved and further diluted in DMSO. The final DMSO concentration did not exceed 1%, a concentration verified not to interfere with the experiments performed.

Pre-evaluation of cytotoxicity was measured using the MTT assay according to literature.[52] Cells were treated with compounds for 24 h. Afterwards 5 mg/mL MTT was added and incubated for 1 h at 37 °C. In order to dissolve the insoluble purple formazan product DMSO was added. The absorbance of the coloured solution was quantified by measuring at 544 nm in a 96-well plate reader (Chameleon Plate, Hidex, Turku, Finland).

Quantification of apoptosis was performed as described by the group of Nicoletti.[53] Briefly, cells were incubated for 24 h with compounds. Afterwards cells were incubated for 2 h (X-Jurkat) or overnight (S-Jurkat) at 4 °C in a hypotonic buffer (0.1% sodium citrate, 0.1% Triton-X-100 and 50 μg/mL propidium iodide) and analyzed by flow cytometry on a FACSCalibur (Becton Dickinson, Heidelberg, Germany). Nuclei to the left of the G_0/G_1 peak were considered as apoptotic cells. The fractional product analysis was employed to assess synergy in treatment effects as recommended in literature.[54]

For western blot analysis cells were collected by centrifugation and lyzed in 1% Triton X-100, 0.15 M NaCl, and 30 mM Tris–HCl (pH7.5) with the proteases inhibitor cocktail complete (Roche, Mannheim, Germany) for 0.5 h. Afterwards lysates were centrifuged at 10,000 g for 10 min. at 4 °C. Proteins were separated by SDS–PAGE and transferred to nitrocellulose membrane (Invitrogen, Karlsruhe, Germany). Membranes were blocked for 1 h with 5% non-fat milk in 0.1% Tween-20/PBS and incubated over night with primary antibody against caspase-9 (rabbit polyclonal antibody; Cell Signaling, Frankfurt, Germany) and actin (maus monoclonal antibody; Millipore, Schwalbach, Germany). Proteins were visualised using secondary antibodies conjugated to horseradish peroxidise and ECL Plus solution (Amersham Bioscience, Freiburg, Germany). Membranes were exposed to X-ray film and developed in a Curix 60 Developing processor (Agfa, Cologne, Germany).

For the determination of XIAP BIR3 binding activity, a sensitive in vitro binding assay using the fluorescence polarization (FP)-based method, was performed as described in literature.[10] Briefly, dose-dependent binding experiments were carried out with serial dilutions of the tested compounds. An aliquot of the samples and preincubated XIAP BIR3 protein (0.030 μM) and fluorescently tagged peptide named SM5F (5 nM) in the assay buffer (100 mM potassium phosphate, pH 7.5; 100 μg/mL bovine gamma globulin; 0.02% sodium azide, purchased from Invitrogen Life Technology), were added to Microfluor 96-well, black, round-bottom plates. For each assay, the controls included XIAP BIR3 protein and SM5F (equivalent to 0% inhibition), and SM5F only (equivalent to 100% inhibition). The polarization values were measured after 3 h of incubation using an ULTRA READER (Tecan U.S. Inc., Research Triangle Park, NC). IC_{50} values (the inhibitor concentration at

which 50% of the bound tracer is displaced) were determined from a plot using nonlinear least-squares analysis.

4.10. Statistical analysis

All pharmacological experiments were performed at least two times in triplicate. Results are expressed as mean value ± SEM. Curve fitting and one way analysis of variance (ANOVA) with Bonferroni's multiple comparison test were performed using GRAPHPAD PRISM software (GraphPad Software, Inc., San Diego, CA). *P* values <0.05 were considered significant.

Acknowledgement

This work was supported by the COMET Center ONCOTYROL and in part funded by the Federal Ministry for Transport Innovation and Technology (BMVIT) and the Federal Ministry of Economics and Labour/the Federal Ministry of Economy, Family and Youth (BMWA/BMWFJ), the Tiroler Zukunftsstiftung (TZS) and the State of Styria represented by the Styrian Business Promotion Agency (SFG). The authors are grateful to P. Schneider for HPLC-SPE-NMR measurements.

Supplementary data

Supplementary data (the 1D and 2D NMR spectra of compounds **4** and **5**) associated with this article can be found, in the online version, at doi:10.1016/j.bmc.2010.10.046.

References and notes

1. Hengartner, M. O. *Nature* **2000**, *407*, 770–776.
2. Sun, C.; Cai, M.; Meadows, R. P.; Xu, N.; Gunasekera, A. H.; Herrmann, J.; Wu, J. C.; Fesik, S. W. *J. Biol. Chem.* **2000**, *275*, 33777–33781.
3. Wu, G.; Chai, J.; Suber, T. L.; Wu, J.-W.; Du, C.; Wang, X.; Shi, Y. *Nature* **2000**, *408*, 1008–1012.
4. Dean, E.; Jodrell, D.; Connolly, K.; Danson, S.; Jolivet, J.; Durkin, J.; Morris, S.; Jowle, D.; Ward, T.; Cummings, J.; Dickinson, G.; Aarons, L.; LaCasse, E.; Robson, L.; Dive, C.; Ranson, M. *J. Clin. Oncol.* **2009**, *27*, 1660–1666.
5. Schimmer, A. D.; Estey, E. H.; Borthakur, G.; Carter, B. Z.; Schiller, G. J.; Tallman, M. S.; Altman, J. K.; Karp, J. E.; Kassis, J.; Hedley, D. W.; Brandwein, J.; Xu, W.; Mak, D. H.; LaCasse, E.; Jacob, C.; Morris, S. J.; Jolivet, J.; Andreeff, M. *J. Clin. Oncol.* **2009**, *27*, 4741–4746.
6. Oost, T. K.; Sun, C.; Armstrong, R. C.; Al-Assaad, A.-S.; Betz, S. F.; Deckwerth, T. L.; Ding, H.; Elmore, S. W.; Meadows, R. P.; Olejniczak, E. T.; Oleksijew, A.; Oltersdorf, T.; Rosenberg, S. H.; Shoemaker, A. R.; Tomaselli, K. J.; Zou, H.; Fesik, S. W. *J. Med. Chem.* **2004**, *47*, 4417–4426.
7. Huang, J.-W.; Zhang, Z.; Wu, B.; Cellitti, J. F.; Zhang, X.; Dahl, R.; Shiau, C.-W.; Welsh, K.; Emdadi, A.; Stebbins, J. L.; Reed, J. C.; Pellecchia, M. *J. Med. Chem.* **2008**, *51*, 7111–7118.
8. Sun, H.; Stuckey, J. A.; Nikolovska-Coleska, Z.; Qin, D.; Meagher, J. L.; Qiu, S.; Lu, J.; Yang, C.-Y.; Saito, N. G.; Wang, S. *J. Med. Chem.* **2008**, *51*, 7169–7180.
9. Sun, H.; Nikolovska-Coleska, Z.; Chen, J.; Yang, C.-Y.; Tomita, Y.; Pan, H.; Yoshioka, Y.; Krajewski, K.; Roller, P. P.; Wang, S. *Bioorg. Med. Chem. Lett.* **2005**, *15*, 793–797.
10. Nikolovska-Coleska, Z.; Xu, L.; Hu, Z.; Tomita, Y.; Li, P.; Roller, P. P.; Wang, R.; Fang, X.; Guo, R.; Zhang, M.; Lippman, M. E.; Yang, D.; Wang, S. *J. Med. Chem.* **2004**, *47*, 2430–2440.
11. Harvey, A. L. *Drug Discovery Today* **2008**, *13*, 894–901.
12. Newman, D. J.; Cragg, G. M. *J. Nat. Prod.* **2007**, *70*, 461–477.
13. Feher, M.; Schmidt, J. M. *J. Chem. Inf. Comput. Sci.* **2003**, *43*, 218–227.
14. Verdine, G. L. *Nature* **1996**, *384*, 11–13.
15. Rollinger, J. M.; Langer, T.; Stuppner, H. *Planta Med.* **2006**, *72*, 671–678.
16. Pfisterer, P. H.; Wolber, G.; Efferth, T.; Rollinger, J. M.; Stuppner, H. *Curr. Pharm. Des.* **2010**, 1718–1741.
17. Ito, H.; Kobayashi, E.; Takamatsu, Y.; Li, S.-H.; Hatano, T.; Sakagami, H.; Kusama, K.; Satoh, K.; Sugita, D.; Shimura, S.; Itoh, Y.; Yoshida, T. *Chem. Pharm. Bull.* **2000**, *48*, 687–693.
18. Taniguchi, S.; Imayoshi, Y.; Kobayashi, E.; Takamatsu, Y.; Ito, H.; Hatano, T.; Sakagami, H.; Tokuda, H.; Nishino, H.; Sugita, D.; Shimura, S.; Yoshida, T. *Phytochemistry* **2002**, *59*, 315–323.
19. Ito, H.; Kobayashi, E.; Li, S.-H.; Hatano, T.; Sugita, D.; Kubo, N.; Shimura, S.; Itoh, Y.; Tokuda, H.; Nishino, H.; Yoshida, T. *J. Agric. Food Chem.* **2002**, *50*, 2400–2403.
20. Banno, N.; Akihisa, T.; Tokuda, H.; Yasukawa, K.; Taguchi, Y.; Akazawa, H.; Ukiya, M.; Kimura, Y.; Suzuki, T.; Nishino, H. *Biol. Pharm. Bull.* **2005**, *28*, 1995–1999.
21. Wu, P.-P.; Kuo, S.-C.; Huang, W.-W.; Yang, J.-S.; Lai, K.-C.; Chen, H.-J.; Lin, K.-L.; Chiu, Y.-J.; Huang, L.-J.; Chung, J.-G. *Anticancer Res.* **2009**, *29*, 1435–1442.
22. Jeong, J. C.; Kim, M. S.; Kim, T. H.; Kim, Y. K. *Neurochem. Res.* **2009**, *34*, 991–1001.
23. Siegelin, M. D.; Reuss, D. E.; Habel, A.; Herold-Mende, C.; von Deimling, A. *Mol. Cancer Ther.* **2008**, *7*, 3566–3574.
24. Choi, Y. H.; Baek, J. H.; Yoo, M.-A.; Chung, H.-Y.; Kim, N. D.; Kim, K.-W. *Int. J. Oncol.* **2000**, *17*, 565–571.
25. Lee, S.-S.; Lin, H.-C.; Chen, C.-K. *Phytochemistry* **2008**, *69*, 2347–2353.
26. Wang, G.-J.; Tsai, T.-H.; Lin, L.-C. *Phytochemistry* **2007**, *68*, 2455–2464.
27. Fiorini, C.; David, B.; Fourasté, I.; Vercauteren, J. *Phytochemistry* **1998**, *47*, 821–824.
28. Kawahara, N.; Satake, M.; Goda, Y. *Chem. Pharm. Bull.* **2002**, *50*, 1619–1620.
29. Jones, G.; Willett, P.; Glen, R. C.; Leach, A. R.; Taylor, R. *J. Mol. Biol.* **1997**, *267*, 727–748.
30. Wolber, G.; Dornhofer, A. A.; Langer, T. *J. Comput. Aided Mol. Des.* **2007**, *20*, 773–788.
31. Wolber, G.; Langer, T. *J. Chem. Inf. Model.* **2005**, *45*, 160–169.
32. Jung, H. A.; Park, J. C.; Chung, H. Y.; Kim, J.; Choi, J. S. *Arch. Pharm. Res.* **1999**, *22*, 213–218.
33. Chen, Z.; Zhang, L.; Chen, G. *J. Chromatogr., A.* **2008**, *1193*, 178–181.
34. Kuo, Y.-C.; Lu, C.-K.; Huang, L.-W.; Kuo, Y.-H.; Chang, C.; Hsu, F.-L.; Lee, T.-H. *Planta Med.* **2005**, *71*, 412–415.
35. Otsuka, N.; Liu, M.-H.; Shiota, S.; Ogawa, W.; Kuroda, T.; Hatano, T.; Tsuchiya, T. *Biol. Pharm. Bull.* **2008**, *31*, 1794–1797.
36. Liu, M.-H.; Otsuka, N.; Noyori, K.; Shiota, S.; Ogawa, W.; Kuroda, T.; Hatano, T.; Tsuchiya, T. *Biol. Pharm. Bull.* **2009**, *32*, 489–492.
37. Kim, Y.-K.; Kim, Y. S.; Choi, S. U.; Ryu, S. Y. *Arch. Pharm. Res.* **2004**, *27*, 44–47.
38. Manach, C.; Scalbert, A.; Morand, C.; Remesy, C.; Jimenez, L. *Am. J. Clin. Nutr.* **2004**, *79*, 727–747.
39. Leung, H. W. C.; Lin, C.-J.; Hour, M.-J.; Yang, W.-H.; Wang, M.-Y.; Lee, H.-Z. *Food Chem. Toxicol.* **2007**, *45*, 2005–2013.
40. Bestwick, C. S.; Milne, L.; Duthie, S. J. *Chem. Biol. Interact.* **2007**, *170*, 76–85.
41. Nadova, S.; Miadokova, E.; Cipak, L. *Neoplasma* **2007**, *54*, 202–206.
42. Sharma, V.; Joseph, C.; Ghosh, S.; Agarwal, A.; Mishra, M. K.; Sen, E. *Mol. Cancer Ther.* **2007**, *6*, 2544–2553.
43. Yoshida, T.; Konishi, M.; Horinaka, M.; Yasuda, T.; Goda, A. E.; Taniguchi, H.; Yano, K.; Wakada, M.; Sakai, T. *Biochem. Biophys. Res. Commun.* **2008**, *375*, 129–133.
44. Berman, H. M.; Westbrook, J.; Feng, Z.; Gilliland, G.; Bhat, T. N.; Weissig, H.; Shindyalov, I. N.; Bourne, P. E. *Nucleic Acids Res.* **2000**, *28*, 235–242.
45. Oost, T. K.; Sun, C.; Armstrong, R. C.; Al-Assaad, A. S.; Betz, S. F.; Deckwerth, T. L.; Ding, H.; Elmore, S. W.; Meadows, R. P.; Olejniczak, E. T.; Oleksijew, A.; Oltersdorf, T.; Rosenberg, S. H.; Shoemaker, A. R.; Tomaselli, K. J.; Zou, H.; Fesik, S. W. *J. Med. Chem.* **2004**, *47*, 4417–4426.
46. Kipp, R. A.; Case, M. A.; Wist, A. D.; Cresson, C. M.; Carrell, M.; Griner, E.; Wiita, A.; Albiniak, P. A.; Chai, J.; Shi, Y.; Semmelhack, M. F.; McLendon, G. L. *Biochemistry* **2002**, *41*, 7344–7349.
47. Park, C. M.; Sun, C.; Olejniczak, E. T.; Wilson, A. E.; Meadows, R. P.; Betz, S. F.; Elmore, S. W.; Fesik, S. W. *Bioorg. Med. Chem. Lett.* **2005**, *15*, 771–775.
48. Smellie, A.; Kahn, S.; Teig, S. *J. Chem. Inf. Comput. Sci.* **1995**, *35*, 285–294.
49. Smelli, A.; Teig, S. L.; Towbin, P. *J. Comput. Chem.* **1995**, *16*, 171–187.
50. Wilkinson, J. C.; Cepero, E.; Boise, L. H.; Duckett, C. S. *Mol. Cell. Biol.* **2004**, *24*, 7003–7014.
51. Chung, S.-K.; Kim, Y.-C.; Takaya, Y.; Terashima, K.; Niwa, M. *J. Agric. Food Chem.* **2004**, *52*, 4664–4668.
52. Mosmann, T. *J. Immunol. Methods* **1983**, *65*, 55–63.
53. Nicoletti, I.; Migliorati, G.; Pagliacci, M. C.; Grignani, F.; Riccardi, C. *J. Immunol. Methods* **1991**, *139*, 271–279.
54. Greco, W. R.; Bravo, G.; Parsons, J. C. *Pharmacol. Rev.* **1995**, *47*, 331–385.